



ELSEVIER

Journal of Wind Engineering
and Industrial Aerodynamics 91 (2003) 1301–1328

JOURNAL OF
wind engineering
AND
industrial
aerodynamics

www.elsevier.com/locate/jweia

Gust loading factor—past, present and future

Ahsan Kareem*, Yin Zhou

*NatHaz Modeling Laboratory, Department of Civil Engineering and Geological Sciences,
University of Notre Dame, Rm. 156, Fitzpatrick Hall, Notre Dame, IN 46556-0767, USA*

Abstract

Wind loads on structures under the buffeting action of wind gusts have traditionally been treated by the “gust loading factor” (GLF) method in most major codes and standards around the world. In this scheme, the equivalent-static wind loading used for design is equal to the mean wind force multiplied by the GLF. Although the traditional GLF method ensures an accurate estimation of the displacement response, it may fall short in providing a reliable estimate of other response components. To overcome this shortcoming, a more consistent procedure for determining design loads on tall structures is proposed. This paper highlights an alternative model, in which the GLF is based on the base bending moment rather than the displacement. The expected extreme base moment is computed by multiplying the mean base moment by the proposed GLF. The base moment is then distributed to each floor in terms of the floor load in a format that is very similar to the one used to distribute the base shear in earthquake engineering practice. In addition, a simple relationship between the proposed base moment GLF and the traditional GLF is derived, which makes it convenient to employ the proposed approach while utilizing the existing background information. Numerical examples are presented to demonstrate the efficacy of the proposed procedure in light of the traditional approach. This paper also extends the new framework for the formulation of wind load effects in the acrosswind and torsional directions along the “GLF” format that has generally been used for the alongwind response. A 3D GLF concept is advanced, which draws upon a database of aerodynamic wind loads on typical tall buildings, a mode shape correction procedure and a more realistic formulation of the equivalent-static wind loads and their effects. A numerical example is presented to demonstrate the efficacy of the proposed procedure in light of the traditional approach. It is envisaged that the proposed formulation will be most appropriate for inclusion in codes and standards.

© 2003 Elsevier Ltd. All rights reserved.

Keywords: Gust factor; Wind loads; Dynamics; Tall buildings; Wind tunnel; Codes and standards

*Corresponding author. Tel.: +574-631-5380; fax: +574-631-9236.

E-mail address: kareem@nd.edu (A. Kareem).

1. Background

The diversity of structures that are sensitive to the effects of wind and the increasing need to improve the performance of constructed facilities have placed a growing importance on the problem of wind effects on structures. Wind loads on structures under the buffeting action of wind gusts have traditionally been treated by the “gust loading factor” (GLF) method in most major codes and standards around the world originally proposed in [1]. In this scheme, the equivalent-static wind loading used for design is equal to the mean wind force multiplied by the GLF. The GLF accounts for the dynamics of wind fluctuations and any load amplification introduced by the building dynamics. Since its introduction, several formulations of the GLF have been advanced, details can be found in [2–6]. Because of its simplicity, the GLF method has received a widespread acceptance around the world and is employed in wind loading codes and standards in almost all major countries (e.g., Australian; Canada; USA; Japan; Europe [7,16,31,39,40]). It should be pointed out that the AS1170.2-89 [7] and the ACI Standard [8] apply the GLF to the base bending moment (BBM); however, the GLF is based on the traditional definition.

Despite its simplicity and many advantages, it is noted that the current GLF-based formulation has two shortcomings. The first limitation specifically concerns the use of this format for analyzing relatively long, tall and flexible structures. It is worth noting that relatively stiffer structures may also be affected by the potential inaccuracy in the distribution of the background loading component. Although the gust factor was originally defined for any load effect, it is actually based on the displacement response, i.e., the gust factor is essentially the ratio between the extreme and the mean displacement response and referred to as DGLF in the subsequent discussion. The DGLF is used indiscriminately for any response component in practice, which may yield inaccurate estimates. Because only the fluctuating and mean displacement responses in the first mode are included in the derivation, the gust factor is constant for a given structure. When a constant gust factor, i.e., independent of height is used for estimating the extreme equivalent wind loading, its distribution is the same as that of the mean wind loading. This contradicts the common understanding of the equivalent wind loads on tall, long and flexible structures. For this type of structures, the resonant response is the dominant one. Therefore, the distribution of the equivalent wind loads should depend on the structural mass distribution and mode shape. Zhou et al. [9] have noted that the GLF method provides an accurate assessment of the structural displacement, but results in less accurate estimation of other response quantities, such as, the base shear force. Second, the GLF method is not valid if either the mean wind force or the mean response is zero, an observation that has been made by others as well. For example, in the case of a cantilever bridge with an asymmetrical first mode shape, the DGLF cannot be defined since the mean displacement response in the first mode is equal to zero [10].

Using the influence functions, Davenport [11] and Drybre and Hansen [12] have developed revised GLF concept and procedure, which are based on the response related to the influence function, but not limited to the displacement. Holmes [3]

presents a detailed treatment of GLF for a range of applications. These developments have resulted in a definite improvement since these procedures would ensure an accurate estimation of the response involved. However, the response-specific GLF also has shortcomings since each response component requires a separate GLF and in the case of zero mean response, this approach fails like the conventional one. More recently, Chen and Kareem [13] have proposed an equivalent-static load representation that linearly combines the background and resonant loads. These loading components are derived using the concept of gust loading envelope and the distribution of inertial loads. The proposed background load based on the gust loading envelope offers a very simplified load description in comparison with the load-response-correlation approach [14] whose spatial distribution exhibits dependence on the response component of interest. It also provides a physically more meaningful and efficacious description of the loading as compared to the gust response factor approach.

This paper highlights an alternative format, in which the GLF is based on the BBM rather than the displacement [15]. The expected extreme base moment is computed by multiplying the mean base moment by the new GLF. The base moment is then distributed to each floor in terms of the floor load in a format that is very similar to the one used to distribute the base shear in earthquake analysis practice. In addition, a simple relationship between the new base moment GLF and the traditional GLF is derived, which makes it convenient to employ the new approach while utilizing the existing background information. A numerical example is presented to demonstrate the efficacy of the proposed procedure in light of the traditional approach.

In this paper, the new framework has been extended to formulate wind load effects in the acrosswind and torsional directions along the “GLF” format, which has generally been used for the alongwind response. In order to overcome the barriers to the adaptation of the gust loading approach for the acrosswind and torsional directions, the proposed scheme draws upon a database of aerodynamic wind loads on typical tall buildings, a mode shape correction procedure and a more realistic formulation of the equivalent-static wind loads and their effects on structures. A numerical example is presented to illustrate the convenience and effectiveness of the proposed procedure in design. It is envisaged that the proposed formulation will be most appropriate for inclusion in codes and standards.

2. Displacement gust loading factor (DGLF)

For the sake of comparison and completeness, the traditional DGLF approach is briefly outlined here [1]. In the DGLF approach, the peak load is given by

$$\hat{P}(z) = G \cdot \bar{P}(z), \quad (1)$$

where G is the gust factor, which takes into account the dynamics of gusts and the structure; and $\bar{P}(z)$ the mean wind force.

In the DGLF approach, G is evaluated in terms of the displacement response

$$G_Y = \hat{Y}(z)/\bar{Y}(z), \quad (2)$$

where G_Y is the DGLF; \bar{Y} the mean displacement; and \hat{Y} the expected extreme displacement response. For a stationary process, G_Y is given by

$$G_Y = 1 + g_Y \sigma_Y(z)/\bar{Y}(z) = 1 + 2g_Y I_H \sqrt{B + R} \quad (3)$$

in which g_Y is the displacement peak factor; σ_Y the root mean square (RMS) displacement; B and R the background and resonant response factors, respectively; and $I_H = \sigma_u/\bar{U}_H$ the turbulent intensity evaluated at the top of the structure. The mean wind load is given by

$$\bar{P}(z) = 1/2\rho C_D W \bar{U}_H^2(z/H)^{2\alpha} \quad (4)$$

in which ρ is the air density; C_D the drag coefficient; W the width of the structure normal to the oncoming wind; $\bar{U}(z) = \bar{U}_H(z/H)^\alpha$ the mean wind velocity at height z above the ground, where \bar{U}_H is the mean wind velocity evaluated at the top height of the structure, H ; and α the exponent of the mean wind velocity profile.

Alternatively, (3) can be expressed in terms of peak factors associated with the background and resonant response as given in ASCE 7-98 [16]

$$G_Y = 1 + 2I_H \sqrt{g_u^2 \cdot B + g_R^2 \cdot R}, \quad (5)$$

where g_u is the wind velocity peak factor; g_R the resonant peak factor. For a Gaussian process $g_R = \sqrt{2 \ln(f_1 T)} + 0.5772/\sqrt{2 \ln(f_1 T)}$ in which T is the observation time, and f_1 the natural frequency of the first mode; and $R = SE/\zeta$ where S is the size reduction factor, E the gust energy factor, and ζ the critical damping ratio of the first mode.

All traditional formulations of the DGLF are based on preceding expressions, but differ in their modeling of turbulence and structural models. These details have led to variations in the prediction of gust factors derived from different DGLF formulations [17]. The coefficients B , E and S are provided graphically in some codes or in a closed form in others (e.g., [1,4,6,18]).

Eq. (5) can be rewritten in terms of mean, background and resonant components, as

$$G_Y = 1 + \sqrt{G_{YB}^2 + G_{YR}^2}, \quad (6)$$

where G_{YB} and G_{YR} are the background and resonant components of the DGLF, respectively.

Usually, the mean structural displacement can be approximated well by the first mode mean displacement response

$$\bar{Y}(z) = \bar{P}_1^*/k_1^* \cdot \varphi_1(z), \quad (7)$$

where $\bar{P}_1^* = \int_0^H \bar{P}(z)\varphi_1(z) dz$, $k_1^* = (2\pi f_1)^2 m_1^*$ and $m_1^* = \int_0^H m(z)\varphi_1^2(z) dz$ are the generalized load, stiffness and mass of the first mode, respectively; the fundamental

mode shape can be approximated by

$$\varphi_1(z) = c(z/H)^\beta \tag{8}$$

in which c and β are constants; and the mass is assumed to be linearly distributed as

$$m(z) = m_0(1 - \lambda(z/H)) \tag{9}$$

in which λ is the mass reduction factor.

The fluctuating displacement can also be approximated with that in the first mode

$$\sigma_Y(z) = \left(\int_0^\infty S_{\xi_1}(f) df \right)^{1/2} \cdot \varphi_1(z), \tag{10}$$

where $S_{\xi_1}(f)$ is the PSD of the fluctuating generalized displacement, which can be computed following the approach given by Davenport [1] as shown in Fig. 1(a)

$$S_{\xi_1}(f) = \int_0^\infty S_u(f) \cdot \chi(\beta, f) \cdot |H_d(f)|^2 df, \tag{11}$$

where $S_u(f)$ is the PSD of the fluctuating wind velocity; χ the aerodynamic admittance function (not in the strict sense, similar to the mechanical admittance) that relates the wind velocity PSD to the PSD of the resulting fluctuating wind force, $S_{\tilde{p}_1^*}(f)$. Using strip and quasi-steady theories and considering the wind structure in terms of vertical and horizontal correlations while ignoring the correlation between wind pressures on windward and leeward surfaces, the following relationship can be obtained:

$$S_{\tilde{p}_1^*}(f) = \chi(\beta, f) \cdot S_u(f), \tag{12}$$

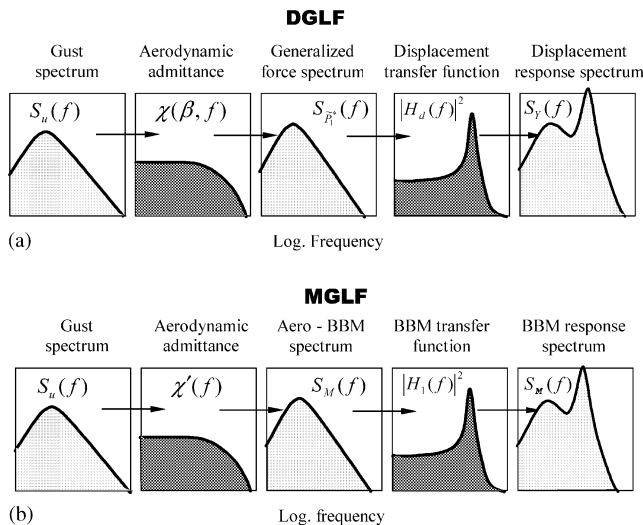


Fig. 1. Probabilistic-dynamics-based approaches to gust loading: (a) DGLF model; and (b) MGLF model [15].

where

$$\chi(\beta, f) = \frac{(\rho C_D WH \bar{U}_H)^2}{(1 + \alpha + \beta)^2} \cdot |J_X(f)|^2 \cdot |J_Z(\alpha, \beta, f)|^2 \quad (13)$$

and

$$|J_X(f)|^2 = \frac{1}{W^2} \int_0^W \int_0^W R_X(x_1, x_2, f) dx_1 dx_2, \quad (14)$$

$$|J_Z(\alpha, \beta, f)|^2 = \frac{(1 + \alpha + \beta)^2}{H^2} \int_0^H \int_0^H \left(\frac{z_1}{H}\right)^{\alpha+\beta} \left(\frac{z_2}{H}\right)^{\alpha+\beta} R_Z(z_1, z_2, f) dz_1 dz_2 \quad (15)$$

are the joint acceptance functions in the horizontal and vertical directions, respectively; $R_X(x_1, x_2, f) = \exp(-(C_X f / \bar{U}(h))|x_1 - x_2|)$ and $R_Z(z_1, z_2, f) = \exp(-(C_Z f / \bar{U}(h))|z_1 - z_2|)$ are the horizontal and vertical coherence functions of the fluctuating wind pressures, respectively; C_X , C_Z the exponential decay coefficients; and h the reference height. Note that based upon the formulation in Fig. 1(a), the aerodynamic admittance is a function of not only the turbulence characteristics and the architectural shape, but also the mode shape. The mechanical admittance function for the first mode displacement response is

$$|H_d(f)|^2 = |H_1(f)|^2 / k_1^{*2} \quad (16)$$

in which

$$|H_1(f)|^2 = \frac{1}{[1 - (f/f_1)^2]^2 + (2\zeta f/f_1)^2}. \quad (17)$$

Using (3) and (10), the fluctuating component of the DGLF can be computed by

$$\sigma_Y(z) / \bar{Y}(z) = \left(\int_0^\infty S_{\bar{P}_1^*}(f) |H_1(f)|^2 df \right)^{1/2} / \bar{P}_1^*, \quad (18)$$

which shows that the DGLF is independent of the mass.

To facilitate engineering computation, (18) is usually treated by dividing the integration into the background and resonant portions. The background and resonant components of the DGLF can be expressed, respectively, by

$$G_{YB} = 2g_u I_H \sqrt{B}, \quad (19)$$

$$G_{YR} = 2g_R I_H \sqrt{R}, \quad (20)$$

where $B = \int_0^\infty \kappa(\beta, f) S_u^*(f) df$ and $R = SE/\zeta$ are the background and resonant response factors, respectively; $\kappa(\beta, f) = ((2 + 2\alpha)/(1 + \alpha + \beta))^2 \cdot |J_X(f)|^2 |J_Z(\alpha, \beta, f)|^2$, which fulfills the function of the aerodynamic admittance; $S = \kappa(\beta, f_1)$ the size reduction factor; $E = (\pi f_1/4) S_u^*(f_1)$ the gust energy factor; $S_u^*(f)$ the normalized wind velocity spectrum with respect to the mean square fluctuating wind velocity, σ_u^2 ; and $I_H = \sigma_u / \bar{U}_H$ the turbulent intensity evaluated at the top of the structure. Most codes and standards use a linear mode shape assumption, or $\beta = 1$, the DGLF

components are then

$$G_{YB} = 2g_u I_H 0 \frac{2 + 2\alpha}{2 + \alpha} \sqrt{\int_0^\infty |J_X(f)|^2 |J_Z(\alpha, 1, f)|^2 S_u^*(f) df}, \tag{21}$$

$$G_{YR} = 2g_R I_H \frac{2 + 2\alpha}{2 + \alpha} \sqrt{|J_X(f_1)|^2 |J_Z(\alpha, 1, f_1)|^2 \frac{\pi f_1}{4\zeta} S_u^*(f_1)}. \tag{22}$$

3. Moment-based gust loading factor (MGLF)

Unlike the traditional DGLF approach, the new procedure uses a BBM -based GLF or MGLF, which is defined as

$$G_M = \hat{M} / \bar{M}, \tag{23}$$

where G_M is the MGLF; \bar{M} the mean BBM; and \hat{M} the expected extreme BBM response. Similar to the treatment of the DGLF, when considering a stationary Gaussian process, the MGLF can be computed by

$$G_M = 1 + g_M \sigma_{\hat{M}} / \bar{M} \tag{24}$$

in which g_M is the peak factor; and $\sigma_{\hat{M}}$ the RMS BBM response.

The BBM response includes the effects of turbulence-structure interaction, which can be captured by the following mode generalized equations of structural motion:

$$m_1^* \ddot{\xi}_1(t) + c_1^* \dot{\xi}_1(t) + k_1^* \xi_1(t) = \tilde{P}_1^*(t), \tag{25}$$

where m_1^* , c_1^* , k_1^* , \tilde{P}_1^* and ξ_1 are the generalized mass, damping, stiffness, load and displacement in the first mode, respectively. Accordingly, quasi-static generalized wind load; $k_1^* \xi(t)$, can be obtained in terms of the generalized displacement. When this load is applied statically, the corresponding generalized displacement and any other response components are identical to those obtained from a complete dynamic analysis.

Accordingly, referring to (11) and (16), the power spectral density (PSD) of the generalized equivalent-static wind load is given by

$$S_{\tilde{P}_1^*}(f) = k_1^{*2} S_{\xi_1}(f) = S_{\tilde{P}_1^*}(f) |H_1(f)|^2 \tag{26}$$

in which the generalized equivalent-static wind load is $\tilde{P}_1^*(t) = \int_0^H \tilde{P}(z, t) \varphi_1(z) dz$, where $\tilde{P}(z, t)$ is the ESWL. Note that symbols used for the externally applied loads are utilized here for the ESWL and its associations, but are given in boldface to distinguish them from the externally applied loads.

The ESWL, $\tilde{P}(z, t)$, is usually distributed, along the building height, in a manner which differs from the mean or fluctuating externally applied aerodynamic loads. Nonetheless, for a linear mode shape, the following relationships are valid for both the externally applied and the equivalent-static wind loads:

$$\tilde{P}_1^* = \tilde{M} / H, \tag{27}$$

$$\tilde{\mathbf{P}}_1^* = \tilde{\mathbf{M}}/H, \quad (28)$$

where $\tilde{\mathbf{M}}$ and $\tilde{\mathbf{M}}$ are the fluctuating components of the externally applied and the induced BBMs, respectively. It is important to distinguish clearly between the equivalent-static/induced and the aerodynamic/externally applied wind loads. The former includes any amplification resulting from building dynamics. Substituting (27) and (28) into (26) leads to

$$S_{\tilde{\mathbf{M}}}(f) = S_{\tilde{\mathbf{M}}}(f)|H_1(f)|^2. \quad (29)$$

Eq. (29) is utilized here to present a new probabilistic treatment of buffeting as highlighted in Fig. 1(b). Two advantages associated with this concept are: (1) it gives a very concise description of the relationship between the aerodynamic load and the induced wind load effects, which facilitates convenient evaluation of the ESWL; (2) in the traditional formulation, the aerodynamic admittance function is difficult to ascertain from theoretical consideration and therefore has led to significant variability in the response estimates (e.g., [17,19]). This can be attributed to a number of reasons including the role of the strip and quasi-steady theories [20]. In the scheme shown in Fig. 1(a), the aerodynamic admittance is actually the transfer function between the input turbulence and the generalized wind load. The generalized wind load is arbitrary in magnitude depending on the normalization scheme used to define the mode shape, and in this format the aerodynamic admittance also becomes a function of the mode shape as shown in (13)–(15). This complicates the verification of the theoretical formulation with experimental measurements. Whereas, in the new formulation, the aerodynamic admittance function describes the relationship between the input turbulence and the BBM. The latter is realistic and can be ascertained conveniently using effective tools, such as the HFBB technique. Therefore, the existing aerodynamic wind load data can be used to aid in improving the accuracy of the current model. Availability of additional data can further refine the predictions based on this model [17,21].

Rewriting (29) in the following non-dimensional form:

$$\sigma_{\tilde{\mathbf{M}}}/\tilde{\mathbf{M}} = \left(\int_0^\infty S_{\tilde{\mathbf{M}}}(f)|H_1(f)|^2 df \right)^{1/2} / \tilde{\mathbf{M}}. \quad (30)$$

Substituting (30) into (24) and after some mathematical manipulations, the MGLF is given by

$$G_M = 1 + 2I_H \sqrt{g_u^2 \mathbf{B} + g_R^2 \mathbf{R}} = 1 + \sqrt{G_{MB}^2 + G_{MR}^2}, \quad (31)$$

where $G_{MB} = 2I_H g_u \sqrt{\mathbf{B}}$ and $G_{MR} = 2I_H g_R \sqrt{\mathbf{R}}$ are the background and resonant components of the MGLF, respectively; and \mathbf{B} and \mathbf{R} are the background and resonant response factors, respectively. B and R can be conveniently derived following the expression given under (20).

For code application of the MGLF, \mathbf{B} and \mathbf{R} can be obtained from graphs or closed-form expressions like the ones used in the DGLF. However, by employing the simple relationship between the DGLF and the MGLF, as described later, the effort required to obtain the MGLF may be significantly reduced.

In the following section, a detailed derivation of the terms in Eq. (31) is presented for the sake of completeness and as a reference for comparison with the terms in DGLF.

The mean BBM on a building is given by

$$\bar{M} = \int_0^H \bar{P}(z)z \, dz = \frac{1/2\rho C_D W U_H^2 H^2}{2 + 2\alpha} \tag{32}$$

The fluctuating BBM response, like the displacement response, is evaluated in terms of the background and resonant components.

The background base moment can be derived following the expression in [22] by employing the influence coefficient function $i(z) = z$

$$\begin{aligned} \hat{M}_B &= g_u \sqrt{\int_0^\infty \int_0^H \int_0^H \int_0^W \int_0^W (\rho C_D W \bar{U}_H)^2 \left(\frac{z_1}{H}\right)^\alpha \left(\frac{z_2}{H}\right)^\alpha R_Z(f) R_X(f) S_u(f) z_1 z_2 \, dx_1 \, dx_2 \, dz_1 \, dz_2 \, df} \\ &= g_u \frac{I_H \rho \bar{U}_H^2 C_D W H^2}{2 + \alpha} \sqrt{\int_0^\infty S_u^*(f) |J_X(f)|^2 |J_Z(\alpha, 1, f)|^2 \, df} \end{aligned} \tag{33}$$

When expressed in a non-dimensional form, the background component of the MGLF is

$$G_{MB} = \frac{\hat{M}_B}{\bar{M}} = 2g_u I_H \frac{2 + 2\alpha}{2 + \alpha} \cdot \sqrt{\int_0^\infty S_u^*(f) |J_X(f)|^2 |J_Z(\alpha, 1, f)|^2 \, df} \tag{34}$$

Since an influence function is used in (33), the contributions from the higher modes and mode coupling, which have been noted to be non-negligible [23], have been automatically included.

On the other hand, for the resonant component, the equivalent-static wind load is equal to the inertial force. For a wind-excited structure, only the contribution of the resonant response in the first mode is typically considered. Using (8)–(13) and considering a non-linear mode shape and a non-uniform mass distribution, the first mode extreme resonant displacement is given by

$$\begin{aligned} \hat{Y}_R(z) &= g_R \frac{(I_H \rho \bar{U}_H^2 C_D W)}{(2\pi f_1)^2 m_0} \frac{(1 + 2\beta)(2 + 2\beta)}{(1 + \alpha + \beta)[(2 + 2\beta) - \lambda(1 + 2\beta)]} \\ &\quad \times \sqrt{|J_X(f_1)|^2 \cdot |J_Z(\alpha, \beta, f_1)|^2 \cdot \frac{\pi f_1}{4\zeta} S_u^*(f_1)} \cdot \left(\frac{z}{H}\right)^\beta \end{aligned} \tag{35}$$

Note that the displacement along the height follows the mode shape. The corresponding ESWL is given by

$$\begin{aligned} \hat{P}_R(z) &= (2\pi f_1)^2 m(z) \hat{Y}_R(z) = (g_R I_H \rho \bar{U}_H^2 C_D W) \frac{(1 + 2\beta)(2 + 2\beta)}{(1 + \alpha + \beta)[(2 + 2\beta) - \lambda(1 + 2\beta)]} \\ &\quad \times \sqrt{|J_X(f_1)|^2 \cdot |J_Z(\alpha, \beta, f_1)|^2 \cdot \frac{\pi f_1}{4\zeta} S_u^*(f_1)} \cdot \left(1 - \lambda \frac{z}{H}\right) \left(\frac{z}{H}\right)^\beta \end{aligned} \tag{36}$$

It can be observed that the distribution of the ESWL is related to the mode shape and the mass distribution. The BBM induced by the load in (20) can be derived by

$$\hat{M}_R = \int_0^H \hat{P}_R(z)z \, dz (g_R I_H \rho \bar{U}_H^2 C_D W H^2) \frac{(1+2\beta)(2+2\beta)}{(1+\alpha+\beta)[(2+2\beta)-\lambda(1+2\beta)]} \\ \times \frac{[(3+\beta)-\lambda(2+\beta)]}{(3+\beta)(2+\beta)} \sqrt{|J_X(f_1)|^2 \cdot |J_Z(\alpha, \beta, f_1)|^2 \cdot \frac{\pi f_1}{4\zeta} S_u^*(f_1)}. \quad (37)$$

Rewriting in a non-dimensional form, the resonant component of the MGLF is

$$G_{MR} = \frac{\hat{M}_R}{\bar{M}} = 2g_R I_H \frac{(1+2\beta)(2+2\beta)(2+2\alpha)}{(1+\alpha+\beta)[(2+2\beta)-\lambda(1+2\beta)]} \frac{[(3+\beta)-\lambda(2+\beta)]}{(3+\beta)(2+\beta)} \\ \times \sqrt{|J_X(f_1)|^2 \cdot |J_Z(\alpha, \beta, f_1)|^2 \cdot \frac{\pi f_1}{4\zeta} S_u^*(f_1)}. \quad (38)$$

4. Relationship between MGLF and DGLF

A comparison between (30) and (18) and the use of the relationships given in (27) and (28) provides the following relationship:

$$\sigma_{\bar{M}}/\bar{M} = \sigma_Y/\bar{Y}. \quad (39)$$

Substituting (39) into (3) and (24) provides a very meaningful relationship

$$G_M = G_Y. \quad (40)$$

This means effectively that the MGLF is numerically equal to the traditional DGLF, which is prescribed in the current codes and standards for structures with linear mode shapes. This would aid in using the existing procedures in codes and standards for the evaluation of MGLF, thus providing a smooth transition from the currently established procedures to the proposed one.

Nonetheless, it is important to note that the equivalence noted in (40) calls for a linear structural mode shape. Some structures may exhibit a departure from the linear mode shape, which has been addressed by several researchers (e.g., [23,24]). The influence of a non-linear mode shape on the relationship between the MGLF and the DGLF is treated in the following section.

As shown in the preceding derivation of the MGLF, the background component of the MGLF is given by (34) which is identical to (21) that describes the background component of the DGLF. It is noteworthy that this result is consistent with (40). For the background response $|H_1(f)| = 1$, and the background BBM component is exactly the aerodynamic base moment, irrespective of the structural and turbulence characteristics as indicated in (26). Nonetheless, a similar relationship between the resonant components of the MGLF and the DGLF is not that straightforward. However, using (22) and (38), a deviation factor can be defined to relate the resonant

component based on the two approaches

$$\eta_R = \frac{G_{MR}}{G_{YR}} = \frac{(1 + 2\beta)(2 + 2\beta)(2 + \alpha)}{(1 + \alpha + \beta)[(2 + 2\beta) - \lambda(1 + 2\beta)]} \times \frac{[(3 + \beta) - \lambda(2 + \beta)]}{(3 + \beta)(2 + \beta)} \cdot \sqrt{\frac{|J_Z(\alpha, \beta, f_1)|^2}{|J_Z(\alpha, 1, f_1)|^2}} \tag{41}$$

where α is the wind velocity profile exponent; β the mode shape exponent in (8); λ the mass reduction parameter in (9) and J_Z is defined in (15). As noted previously, for a linear mode shape η_R is unity regardless of other parameters.

On the other hand, when the mode shape of the structure is non-linear, the resonant deviation factor is dependent on both the structural and the turbulence characteristics. The effect of correlation of the approaching flow defined in (15) is illustrated in Fig. 2(a). Usually, there is a significant variation in the definition of this correlation function. However, for the two limiting correlation cases, i.e., $C_Z = 0$ (fully correlated) and $C_Z \rightarrow \infty$ (zero-correlated), the correlation effect is within 15% when $\beta = 2.0$. In the general range of $C_Z = 5-15$, this effect is within 5% for $\beta = 0.5-2.0$. Fig. 2(b) shows the effect of a non-linear mode shape on the resonant response deviation factor. Using $C_Z = 11.5$ [6], the effect of a non-linear mode shape is within 5% for $\beta = 0.5-2.0$, and the deviation factor is insensitive to the wind velocity exponent, α . The deviation factor is also insensitive to the mass reduction factor, λ which introduces an error of less than 3% when $\lambda \leq 0.5$, which is a reasonable value for most buildings. The effect of a non-uniform mass distribution is illustrated in Fig. 2(c).

The preceding parameter study shows that the deviation factor is not very sensitive to the variations in the structural and turbulence characteristics. In other words, for a wide range of structural and turbulence characteristics, the resonant MGLF component can be approximated by the resonant DGLF component, resulting usually in slightly conservative estimates of wind loads and associated responses.

5. Design procedure

For design applications, a simplified procedure for estimating the ESWL utilizing the MGLF is presented here.

Step 1: Compute the mean wind force at each floor

$$\bar{P}_i = \left(\frac{1}{2}\rho \bar{U}_H^2 (Z_i/H)^{2\alpha}\right) C_D (W \cdot \Delta H_i), \tag{42}$$

where Z_i is the height of the i th floor above the ground; and $\Delta H_i = Z_i - Z_{i-1}$.

Step 2: Compute the mean BBM

$$\bar{M} = \sum_{i=1}^N \bar{P}_i Z_i, \tag{43}$$

where N is the number of floors of the structure.

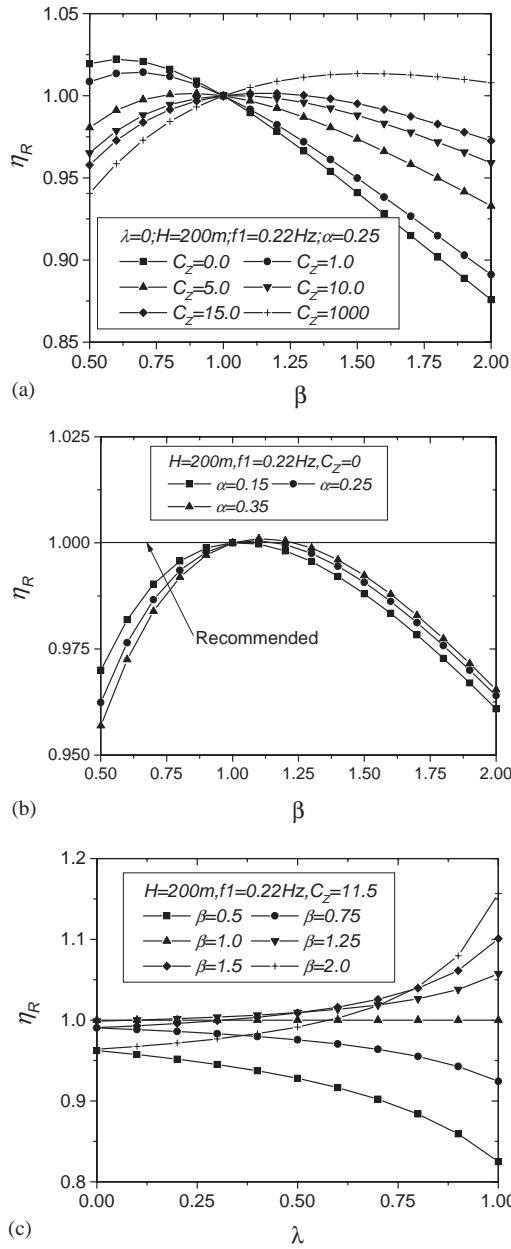


Fig. 2. (a-c) Deviation factor (Eq. 41) for resonant response.

Step 3: Following the guideline of any current code or standard, obtain B , S and E and compute the DGLF using a linear mode shape

$$G_{MB} = G_{YB} = 2g_u I_H \sqrt{B}, \quad (44)$$

$$G_{MR} = G_{YR} = 2g_R I_H \sqrt{SE/\zeta}, \quad (45)$$

$$G_M = 1 + \sqrt{G_{MB}^2 + G_{MR}^2}. \quad (46)$$

Step 4: Compute the resonant extreme BBM component

$$\hat{M}_R = G_{MR} \bar{M}. \quad (47)$$

Step 5: Compute the extreme ESWL at each floor. The resonant component can be obtained by distributing the BBM to each floor as a fraction of the extreme BBM according to

$$\hat{P}_{Ri} = \frac{m_i \varphi_i}{\sum m_i \varphi_i Z_i} \hat{M}_R, \quad (48)$$

where $\varphi_i = \varphi_1(Z_i)$. Note that the distribution of the background ESWL is usually dependent on the response component under consideration and different from the mean and inertial components. Nevertheless, the following description serves as a fairly good approximation [10]:

$$\hat{P}_{Bi} = G_{MB} \bar{P}_i. \quad (49)$$

Step 6: Estimate the extreme responses of interest through a simple static analysis. For example, the extreme displacement response can be computed simply by

$$\hat{Y}_i = G_M \bar{Y}_i \quad (50)$$

and the acceleration at each floor level is given by

$$\hat{a}_i = G_{MR} \cdot \bar{Y}_i \cdot (2\pi f_1)^2. \quad (51)$$

For other response components involving both the resonant and background contributions, e.g., the base shear and other internal forces, the resultant value can be obtained using an SRSS combination rule

$$\hat{r} = \bar{r} + \sqrt{(\hat{r}_B)^2 + (\hat{r}_R)^2}, \quad (52)$$

where \bar{r} , \hat{r}_B and \hat{r}_R are the mean, background and resonant response components obtained from the static structural analysis by employing the above ESWL components separately. The resultant wind-induced response can then be combined with the response under the action of other loads.

5.1. Example

An example building with the following characteristics is used to illustrate the proposed scheme: $H \times W \times D = 200 \times 50 \times 40 \text{ m}^3$; $f_1 = 0.22 \text{ Hz}$; $\zeta = 0.01$; $\varphi_1(z) = (z/H)^\beta$; $m(z) = m_0(1 - \lambda(z/H))$, $m_0 = 5.5 \times 10^5 \text{ kg/m}$; $C_D = 1.3$. The wind

environment is $\bar{U}_{10} = 30$ m/s; $\alpha = 0.15$; $\sigma_u/\bar{U}_{10} = 0.2$ and Davenport spectrum, $C_X = C_Z = 11.5$. Four cases are considered here. In Case 1, $\beta = 1.0$ and $\lambda = 0.0$; in Case 2, $\beta = 1.6$ and $\lambda = 0.0$; in Case 3, $\beta = 1.0$ and $\lambda = 0.2$; and in Case 4, $\beta = 1.6$ and $\lambda = 0.2$.

The mean, background and resonant ESWL components are separately computed using the DGLF method and the proposed MGLF procedure. These wind-loading components are plotted in Fig. 3.

The traditional DGLF method usually does not differentiate the cases that have non-linear mode shapes or non-uniform mass, or both, from the case that has a linear mode shape and uniform mass, or Case 1. Therefore, in the four cases studied here, the DGLF method gives the same result. The mean and background ESWL components obtained using the MGLF procedure are the same as those obtained using the DGLF approach. However, the resonant component is different. Even for Case 1, the ESWL given by the MGLF procedure has a linear distribution, which is clearly different from that given by the traditional method. The latter varies along the height following a 2α exponent law.

Due to the difference in the distribution of the wind loads, the estimated responses will be different. A comparison of different GLFs for different response components by the two procedures is given in Table 1, which includes also the GLF for the base shear in which discrepancies in base shear response estimates were observed. The items in brackets are the ratios between the GLFs obtained by the MGLF procedure and the corresponding GLFs by the DGLF method. By definition, the DGLF method results in a uniform gust factor for all responses and here for all four cases.

For Case 1, the MGLF is, as expected, equal to the DGLF. A non-linear mode shape (Case 2), or a non-uniform mass (Case 3), or both (Case 4) influences the MGLF. However, as was exemplified in the preceding parametric study, the effect of the non-uniform mass is insignificant and the effect of a non-linear mode shape is 2.2% on the resonant MGLF and 0.8% on the resultant MGLF, which are negligible. For Case 4, the error is slightly reduced compared to Case 2.

The MGLF procedure determines the ESWL in a more realistic manner than the traditional DGLF method. Therefore, the resulting response estimates may differ. Using the base shear force as an example, the resonant base shear force by the MGLF procedure is 15% less than that obtained by the DGLF method for Case 1, which resulted in a base shear gust factor that was 5.4% less than the DGLF. For Case 2, the respective errors increase up to 23.2% and 8.3%. Although this effect is on the conservative side for the base shear force, this observation does not necessarily apply to other responses. Due to the difference in the distribution of the wind loading, the deviation in responses estimated by the DGLF method will depend on the response being estimated and the structural characteristics. For example, the resonant ESWL on the top floor obtained by the DGLF method is 33% (350/520 kN) less than the value given by the MGLF procedure for Case 2.

The base shear GLF is more sensitive to the mode shape and mass distribution than the MGLF, and it is always different from the DGLF. In light of this

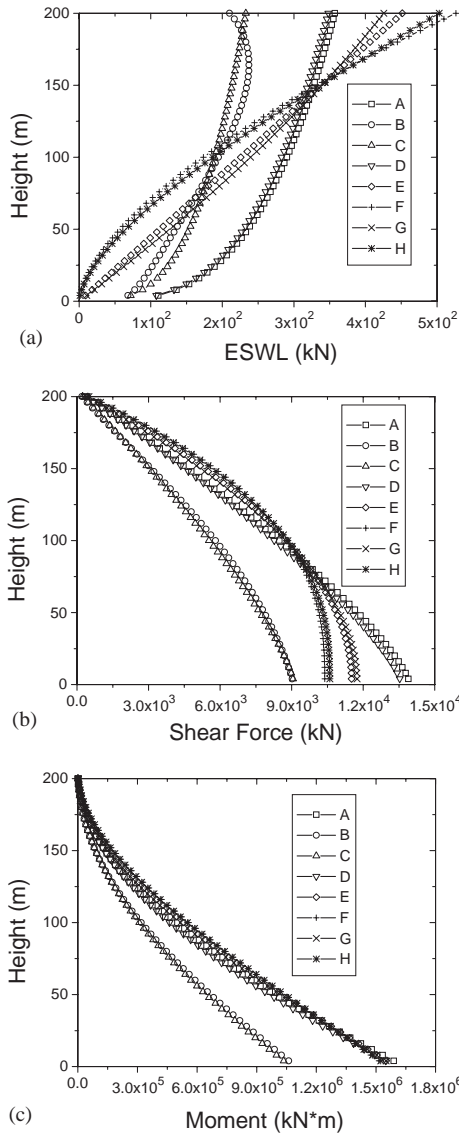


Fig. 3. (a–c) Wind loads/effects using DGLF and MGLF. (A) mean wind force; (B) background ESWL with respect to the BBM response [15]; (C) background ESWL by the DGLF approach; (D) resonant ESWL by the DGLF approach; (E) resonant ESWL by the MGLF procedure for case 1; (F) resonant ESWL by MGLF for case 2; (G) resonant ESWL by MGLF for case 3; and (H) resonant ESWL by MGLF for case 4.

sensitivity, the proposed procedure was not designed to use a base shear force to distribute the ESWL to floors, although this approach is used in earthquake engineering practice.

Table 1
Comparison of gust loading factors

Case	DGLF formulation			MGLF formulation					
	All responses			Base bending moment			Base shear force ^a		
	G_B	G_R	G	G_B	G_R	G	G_B	G_R	G
1	0.652	0.974	2.172	0.652 (1.000) ^b	0.976 (1.002)	2.174 (1.000)	0.652 (1.000)	0.829 (0.851)	2.055 (0.946)
2	0.652	0.974	2.172	0.652 (1.000)	0.953 (0.978)	2.155 (0.992)	0.652 (1.000)	0.748 (0.768)	1.992 (0.917)
3	0.652	0.974	2.172	0.652 (1.000)	0.976 (1.002)	2.174 (1.000)	0.652 (1.000)	0.845 (0.868)	2.067 (0.952)
4	0.652	0.974	2.172	0.652 (1.000)	0.959 (0.985)	2.160 (0.994)	0.652 (1.000)	0.763 (0.783)	2.004 (0.923)

^a GLF for base shear $G = \hat{Q}/\bar{Q}$ where the peak base shear force, \hat{Q} , is computed using actual ESWLs, e.g., Eq. (36) for resonant component; and \bar{Q} is the mean base shear force.

^b Items in brackets are the ratios between wind load effects obtained by the MGLF formulation and those by the DGLF formulation. These ratios are also equal to the ratios of GLFs for wind effects of concern between these two GLF formulations. In the DGLF, the ESWL is determined by (1); while in the MGLF it is by (48) and (49).

6. 3D gust loading factors

The last part of the paper advances the concept of 3D GLF for estimating dynamic load components in three directions [25]. Under the actions of windstorms, actual tall buildings vibrate simultaneously in alongwind, acrosswind and torsional directions. In many cases, the wind-induced response due to acrosswind and torsional excitations is as important as the alongwind in terms of both serviceability and survivability design of tall buildings. Nevertheless, most current codes and standards focus only on procedures for the alongwind response, with little guidance for the other two directions [26,27,41]. Piccardo and Solari [28] reported a 3D closed-form GLF formulation based on a combination of the quasi-steady theory and empirical fit to a general acrosswind spectrum utilizing the DGLF framework.

This section provides a framework for the formulation of those wind load effects along the “GLF” format that has generally been used for the alongwind response. This approach is based on an extension of the new GLF concept provided in the preceding sections to the three response components, a database of aerodynamic wind load on typical tall buildings, a mode shape correction procedure and a more realistic formulation of the equivalent-static wind loads and their effects. It is envisaged that the new formulation will be most appropriate for inclusion in codes and standards and also serves as a convenient format for the interpretation of wind tunnel test results.

The proposed 3D GLF is an extension of a new MGLF concept based on the BBM or base torque response defined as

$$G = \hat{M} / \bar{M}', \quad (53)$$

where G is the GLF; \bar{M}' the reference mean BBM or base torque, which can be computed for the sway and torsional modes, respectively, by

$$\bar{M}'_{D,L} = \int_0^H \bar{P}(z) \cdot z \, dz, \quad (54)$$

$$\bar{M}'_T = \int_0^H \bar{P}(z) (0.04B) \, dz, \quad (55)$$

where $\bar{P}(z)$ is the mean alongwind load at any height z above the ground; and H and B the building height and width normal to the oncoming wind, respectively. Subscripts D, L and T represent the alongwind, acrosswind and torsional directions, respectively. If not specifically indicated, the given formulation would be applicable to all three directions. The reference mean base moment in (54) in the acrosswind and the base torque in (55) are not the actual mean base moments that act on the building. Usually, for most symmetrical buildings, the mean base moments in the acrosswind and torsional directions are either very small or zero. The reference mean torque in (55) corresponds to the overall torsional effect of a partial load with 25% reduction in any portion of the building, as recommended in the current ASCE 7 [16] and NBCC [24,29–32].

For convenience, the reference mean base moment in the acrosswind is set equal to the alongwind mean base moment. \hat{M} is the peak BBM or base torque response which can be expressed as

$$\hat{M} = \bar{M} + g \cdot \sigma_M, \quad (56)$$

where \bar{M} is the mean BBM or base torque; g the peak factor, which is usually around 3–4; and $\sigma_M = (\int_0^\infty S_M(f) \, df)^{1/2}$ the RMS of the BBM and base torque response, and $S_M(f)$ the PSD of the fluctuating base moment or torque response. It has been a general practice to divide the integration term of the fluctuating response into two portions

$$\sigma_M = \sqrt{\sigma_{MB}^2 + \sigma_{MR}^2} \quad (57)$$

in which σ_{MB} and σ_{MR} are the background and resonant components of the BBM or base torque response, respectively. Thus, the 3D GLF in (1) can be expressed in the form

$$G = \bar{G} + \sqrt{G_B^2 + G_R^2}, \quad (58)$$

where \bar{G} , G_B and G_R are the mean, background and resonant components of the GLF, respectively, which can be computed by

$$\bar{G} = \bar{M} / \bar{M}', \quad (59)$$

$$G_B = g_B \cdot \sigma_{MB} / \bar{M}', \quad (60)$$

$$G_R = g_R \cdot \sigma_{MR} / \bar{M}', \quad (61)$$

where $g_B = g_u$ is the background peak factor or peak factor for the fluctuating wind velocity as suggested in ASCE 7 [16]. It is important to note that when applying to the alongwind response, the preceding 3D GLF reduces exactly to the same result as given in a new GLF model by Zhou and Kareem [15]. This new GLF model has the advantage of offering an improved GLF format that reflects more accurately the description of dynamic load effects on structures in comparison with the traditional GLF approach as used in current codes and standards. For the alongwind response, the mean component of the GLF is unity; and for the acrosswind and torsional response of a symmetrical building, it is usually very small or zero. The calculation for the background and resonant components of the **BBM** response will be provided in the following sections based on the background provided in Appendix A.

6.1. Base moments response and mode shape corrections

Most GLF-based approaches involve the generalized wind loading, which has been observed to be quite sensitive to the mode shape exponent and the aerodynamic pressure field characteristics (e.g., [33]). These parameters in engineering practice are either unknown or can only be estimated approximately. For a particular engineering application, the mode shape correction of the generalized wind load scheme may introduce significant uncertainty depending on the parameters involved. On the other hand, it is noted that a **BBM**-based procedure can notably reduce the analysis efforts. The PSD of the fluctuating **BBM** or base torque response can be evaluated using the following equation:

$$S_M(f) = \eta_M \cdot S_M(f) \cdot |H_1(f)|^2, \quad (62)$$

where η_M is the mode shape correction for the base moments and torque response. For the background response, both $|H_1(f)|^2$ and η_M are equal to unity. When a building has an ideal mode shape, i.e., linear in sway modes and uniform in torsional direction, η_M for the resonant response component is also equal to unity [15,24,34]. In addition, studies have shown that, unlike the procedure based on the generalized wind load, the mode shape correction η_M for the base moments is relatively insensitive to the non-ideal mode shape, mass distribution and aerodynamic pressure field characteristics. For a wide range of involved parameters, the mode shape correction can be neglected in the base moments-based approach, which results in acceptable error in the overall wind-induced response estimates [10,24]. It is noteworthy that the same symbol but expressed in bold is employed in (62) to distinguish the base moment or base torque response from the externally applied aerodynamic moment or torque. The former includes the dynamic magnification effects resulting from wind fluctuations and structural dynamics.

Using (62), the definition of the background response, and the white-noise excitation assumption, the background and resonant components of the base

moments can be computed, respectively, by

$$\sigma_{MB} = \sigma_M, \quad (63)$$

$$\sigma_{MR} = \sqrt{\frac{\pi f_1}{4\zeta_1}} \cdot S_M(f_1). \quad (64)$$

6.2. Aerodynamic base moment database

The aerodynamic base moments involve complex fluid-structure interactions, which can only be determined accurately with wind tunnel tests except for the alongwind direction, where the strip and quasi-steady theories are usually assumed. For the acrosswind and torsional directions, there has not been, to date, any acceptable analytical procedure to determine this information based on the oncoming velocity fluctuations and building geometry. The base moment in a non-dimensional form can be obtained from the HFBB [34,35] or simultaneously monitored surface pressure measurements on scaled building models (e.g., [36,37]).

An initial aerodynamic base moment database based on the HFBB measurements is developed and reported in detail in Zhou et al. [21]. The data includes seven rectangular building models, with side ratio (D/B , where D is the depth of the building section along the oncoming wind direction) from 1/3–3, three aspect ratios for each building model in two approaching flows, namely, BL1 ($\alpha = 0.16$) and BL2 ($\alpha = 0.35$), corresponding, respectively, to an open and an urban wind environment. The data are provided and are accessible to the community with a user-friendly Java-based applet through the world-wide-web (<http://www.nd.edu/~nathaz>). With the expedient HFBB, the existing database can be easily expanded [21].

In this database, the measured aerodynamic base moments are reduced in the following non-dimensional formats:

$$\sigma_{CM} = \sigma_M / M', \quad (65)$$

$$C_M(f) = (f \cdot S_M(f)) / \sigma_M^2, \quad (66)$$

where M' is the reference moment or torque in the test, which is defined by $M'_D = (1/2\rho\bar{U}_H^2BH^2)$, $M'_L = (1/2\rho\bar{U}_H^2DH^2)$ and $M'_T = (1/2\rho\bar{U}_H^2BDH)$ for the alongwind, acrosswind and torsional directions, respectively. The non-dimensional data can be directly used in the response analysis of buildings. It is important to note the manner in which the reference moments have been defined in this database, e.g., the acrosswind moment is non-dimensionalized with respect to D , which is the acrosswind face dimension. An example of aerodynamic loads on a square tall building model is given in Fig. 4 for both open country and urban terrains.

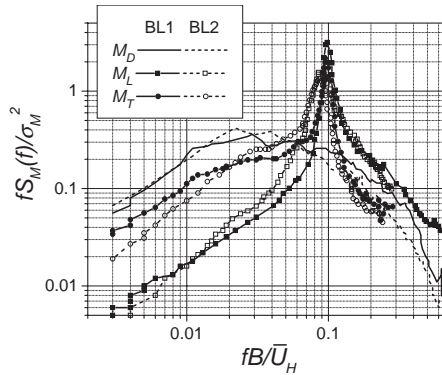


Fig. 4. PSD of the aerodynamic base moments, e.g., building.

6.3. Evaluation of the 3D GLF

Given the aerodynamic base moments, the three components of 3D GLF can be evaluated by substituting (63)–(66) into (59)–(61) as

$$\bar{G} = \begin{cases} 1 & \text{for alongwind,} \\ 0 & \text{for acrosswind and torsion for symmetric buildings,} \end{cases} \quad (67)$$

$$G_B = g_B \cdot \sigma_{CM} \cdot M' / \bar{M}', \quad (68)$$

$$G_R = g_R \frac{\sigma_{CM} \cdot M'}{\bar{M}'} \sqrt{\frac{\pi \cdot C_M(f_1)}{4\zeta_1}}. \quad (69)$$

6.4. Application of 3D GLF in design

Among other advantages, the base moment response-based GLF, as outlined here exhibits a notable feature that the ESWL on a building can be obtained by distributing the base moment response to each floor. For the mean and background components, the ESWLs can be expressed by

$$\bar{P}_i = \bar{M} \cdot \frac{2 + 2\alpha}{H^2} \cdot \left(\frac{z_i}{H}\right)^{2\alpha} \cdot \Delta H_i, \quad (70)$$

$$\hat{P}_{BiD,L} = \hat{M}_{BD,L} \cdot \frac{2 + 2\alpha}{H^2} \cdot \left(\frac{z_i}{H}\right)^{2\alpha} \cdot \Delta H_i, \quad (71)$$

$$\hat{P}_{BiT} = \hat{M}_{BT} \cdot \frac{1 + 2\alpha}{H} \cdot \left(\frac{z_i}{H}\right)^{2\alpha} \cdot \Delta H_i. \quad (72)$$

For the resonant components, the ESWL in sway modes is given by

$$\hat{P}_{RiD,L} = \hat{M}_{RD,L} \cdot \frac{m_i \varphi_{1iD,L}}{\sum m_i z_i \varphi_{1iD,L}} \quad (73)$$

and the torsional mode

$$\hat{\mathbf{P}}_{RiT} = \hat{\mathbf{M}}_{RT} \cdot \frac{I_i \varphi_{1iT}}{\sum I_i \varphi_{1iT}}, \tag{74}$$

where $\bar{\mathbf{P}} = \text{ESWL}$; $\bar{\mathbf{M}} = \bar{\mathbf{G}} \cdot \bar{\mathbf{M}}'$, $\hat{\mathbf{M}}_B = G_B \cdot \bar{\mathbf{M}}'$ and $\hat{\mathbf{M}}_R = G_R \cdot \bar{\mathbf{M}}'$ are the mean, background and resonant base moment components, respectively; z_i the elevation of the i th floor above the ground; $\Delta H_i = z_i - z_{i-1}$ the floor height of the i th floor; and m_i , I_i and φ_{1i} the mass, mass moment of inertia and first mode shape at the i th floor height, respectively.

6.5. Load effects

Any wind load effects such as the internal forces in each member, as well as the overall deflection and acceleration, can be computed expediently through a simple analysis utilizing these ESWLs. For example, the acceleration response estimated for serviceability checking procedure can be evaluated using only the resonant ESWL component

$$\sigma_{ai} = \frac{\sum \hat{\mathbf{P}}_{Ri} \cdot \varphi_{1i}}{g_R \cdot \sum m_i \varphi_{1i}^2} \cdot \varphi_{1i}. \tag{75}$$

6.6. Example

An example tall building is used to demonstrate the efficacy of the scheme presented here. The building is a square steel tall building with size $H \times W1 \times W2 = 200 \times 40 \times 40 \text{ m}^3$ and an average radius of gyration of 18 m. The three fundamental mode frequencies, f_1 , are 0.2, 0.2 and 0.35 Hz in X, Y and Z directions, respectively; the mode shapes are all linear or β is equal to 1.0; and there is no modal coupling. The building density is equal to 250 kg/cu m. This building is located in Exposure A or close to the BL2 test condition of the internet-based database [21]. In this location (exposure A), the reference 3-second design gust speed, U_{10} , at a 50-year recurrence interval is 63 m/s [10,16], which is equal to 18.9 m/s upon conversion to 1-h mean wind speed with 50-year recurrence interval ($63 \times 0.30 = 18.9 \text{ m/s}$). For serviceability requirements, 1-h mean wind speed with 10-year recurrence interval is equal to 13.99 m/s ($63 \times 0.30 \times 0.74 = 13.99$). For the sake of illustration, the first mode critical structural damping ratio, ζ_1 , is assumed to be 0.01 for both survivability and serviceability design as suggested in the ASCE 7-98 standard [16].

Using these aerodynamic data and the procedures provided in this paper, the 3D GLF and wind load effects are evaluated and the results are presented in Table 2. This table includes also the GLF, base moments and acceleration response in the alongwind direction obtained by employing the procedure in ASCE 7-98 [16]. A sampling of floor-level ESWL components are shown in Fig. 5. Only ESWL in sway modes is provided in Fig. 5 due to the relatively insignificant contribution of the torsional component for this building.

Table 2
3D 3GLFs and wind load effects for design

Building and wind direction (1)	Load components (2)	σ_{CM} (3)	Survivability design								Serviceability design					
			Aerodyn. load coef.		GLF and base moments (10e6 kNm)						Aerodyn. load coef.		GLF and Acc. (mg or rad/s ²)			
			f_1^{*a} (4)	$C_M(f_1)$ (5)	\bar{G} (6)	G_B (7)	G_R (8)	G (9)	\bar{M} (10)	\hat{M} (11)	f_1^{*a} (12)	$C_M(f_1)$ (13)	G_R^b (14)	σ_a (15)	Corner	
															X (16)	Y (17)
	D ^c							1.18 ^d	3.28 ^d	3.86			1.53	5.44	6.39 ^e	9.46 ^e
B	D	0.109	0.156	0.048	1.00	0.76	1.64	2.81	1.28	3.61	0.211	0.040	1.50	5.32		
D	L	0.133	0.156	0.192	0.00	0.93	4.01	4.12	1.28	5.28	0.211	0.073	2.47	8.77		
I	T	0.044	0.273	0.059	0.00	4.80	11.93	12.86	0.016	0.21	0.369	0.040	9.83	0.02	3.54 ^f	3.54 ^f

$$^a f_1^{*a} = f_1 B / \bar{U}_H.$$

^b When using procedure in ASCE 7-98, $G_R = 1.7g_R I_z R$ where I_z is the turbulence intensity at the computation height, \bar{z} , and R is a resonance factor.

^c Based on ASCE 7-98 procedure (ASCE 2000).

^d By the ASCE 7 code, the GLF and the mean base moment are evaluated in terms of 3-s gust wind speed; while the estimate of the peak base bending moment is based on 1-h averaging time. All other cases for the GLF, base moments and accelerations using either code procedure or the procedure in this paper are consistently based on 1-h averaging time [27].

^e Resultant acceleration.

^f Acceleration components due to torsional movement, which is $\gamma \cdot \sigma_{aT}$.

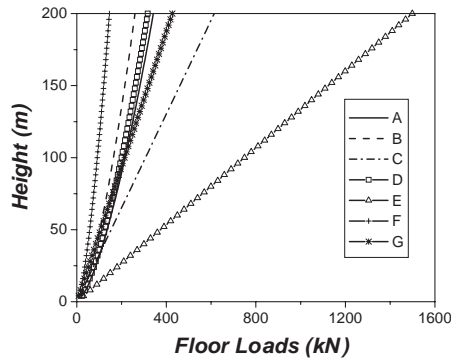


Fig. 5. Floor ESWL components. (A) alongwind mean; (B) alongwind background; (C) alongwind resonant; (D) acrosswind background; (E) acrosswind resonant; (F) torsional background divided by radius of gyration; and (G) torsional resonant divided by radius of gyration.

Generally, for the alongwind load effects, the ASCE [16] code procedure and the proposed GLF format lead to rather close estimates of BBMs and acceleration response. This good agreement between the code procedure that is based on closed-form solutions (e.g., [18]) and the procedure in this paper which utilizes wind tunnel experimental data, confirms the effectiveness of the proposed 3D GLF-based analysis scheme. Meanwhile, following the new GLF format [10,15], the proposed procedure evaluates the ESWL in a more realistic manner in comparison with the code procedure which provides an ESWL that follows the distribution of the mean wind force [1]. The more realistic ESWL by the proposed GLF format, as shown in Fig. 5, will result in more accurate estimates of other wind effects such as shear forces among others [9,10,15].

In the current ASCE 7 standard [16], wind loads and effects can only be evaluated for the alongwind component at each wind direction. However, the scheme presented herein permits capturing of wind load effects in three directions, which represent more closely the actual building motion under wind. It is noteworthy that despite the fact that the total alongwind loading may be dominant in comparison with the acrosswind load for most relatively rigid buildings since the mean wind force in the acrosswind is usually very small, the fluctuating acrosswind wind components may become increasingly important as buildings become more flexible. The acrosswind aerodynamic force spectra usually exhibits apparent peak in amplitude in the vicinity of frequencies of interest for design of tall flexible structures thus may exceed the corresponding alongwind force component. Therefore, the procedure based solely on the alongwind response analysis, as advocated in the current ASCE and other standards may fall short in predicting accurately the wind load effects on flexible structures. Furthermore, the quasi-steady, or background load effects on intermediate height buildings may be significant in defining design load effects and should be given due consideration as advanced in the proposed framework.

Although the mean torsional force is equal to zero in light of the symmetry of the example building plan and rather uniform unobstructed approach flow, the large torsional GLF points at the need for improved guidance in codes and standards to include the contributions from the fluctuating torsional components [24,29,30,32].

7. Concluding remarks

This paper highlights developments in the GLF approach for civil engineering structures from its inception, following the pioneering work of Professor Alan G. Davenport, to modifications that ensued and outlook for the future offered by the new format for the 3D GLFs.

The ESWL derived from the traditional DGLF method may deviate from the actual value, and consequently may lead to unfavorable estimates of some wind-induced load effects. This paper proposes a new procedure for determining the ESWL, which employs a BBM-based GLF or MGLF. The expected extreme BBM is computed by multiplying the mean BBM by the proposed MGLF. The extreme BBM is then distributed to all floors in a format very similar to the one used in earthquake engineering to distribute the base shear. In the case of linear structural mode shape, the proposed MGLF is numerically equal to the traditional DGLF. A parameter study suggests that for cases in which the mode shape and the mass distributions depart from linear and uniform, respectively, a tacit assumption of equivalence between the MGLF and the DGLF would result in slightly conservative estimates of wind loading and associated response. This would enable the use of the existing background information concerning DGLF, in codes and standards, in the proposed procedure.

The proposed MGLF scheme offers several advantages over the DGLF approach. First, it provides the ESWL in a more realistic manner. This is the most important proposed feature of the procedure. Second, it uses the existing information, which permits a smooth transition from the DGLF to the MGLF formulation—a convincing feature for possible adaptation by codes and standards. Third, it is formulated in a format that is familiar to most design engineers. Fourth, a new analysis model, which is based on the BBM, is highlighted. In addition to its advantage in presenting the ESWL correctly, this model is relatively more straightforward than the current displacement-based model in ascertaining the aerodynamic admittance function since the admittance function in this formulation does not depend on the mode shape [17]. Fifth, the application range has been extended to accommodate non-linear mode shapes and non-uniform mass distributions. Sixth, it provides the opportunity for a generalized formulation and a consistent transition in prediction of response for structures ranging from relatively rigid to more flexible. Finally, it offers a foundation for the development of a consistent GLF model for 3D wind effects on tall buildings. The base moment-based analysis and modeling also offers an attractive format for reducing wind tunnel data derived from HFBB and aeroelastic balance [38].

Following the formulation of the new GLF model for the alongwind response, a 3D GLF format for estimating the alongwind, acrosswind and torsional load effects is presented. In light of the current code procedure which is based only on the closed-form alongwind response analysis, the proposed 3D GLF model demonstrates its advantages in terms of its simple and uniform format and ability to capture accurately building motions under wind. The proposed approach also includes the influence of non-ideal mode shapes [9,10] and realistic representation of the ESWL and other wind load effects on the response, utilizes a newly developed aerodynamic wind load database [21] and offers venues for appropriately combining the 3D wind load effects. The proposed 3D GLF model is best suited for codes and standards as a guide in the preliminary design stages. It also serves as a convenient format for interpreting wind tunnel test results using HFBB. The range of application of the proposed model can be conveniently extended with the availability of more HFBB data.

8. Acknowledgements

The authors gratefully acknowledge the partial support from NSF Grants #CMS 95-03779, CMS 95-22145 and CMS 00-85019 for this study. The authors are very thankful to Dr. X. Chen for his comments on the proposed formulation. The authors are indebted to Professor Davenport for his many technical contributions which have been a source of inspiration in their respective careers.

Appendix A. Derivation of resonant and background moment components

Using random vibration, modal and spectral analysis methods, the 3D generalized displacement response of a building excited by wind actions can be computed, in a matrix notation, by

$$[S_{\xi^*}(f)] = [H(2i\pi f)][S_{p^*}(f)][H^*(2i\pi f)]^T, \tag{A.1}$$

where $[S_{\xi^*}(f)]$ is the spectral density matrix of generalized displacement response, with usually only those in three fundamental modes are considered; $[H(2i\pi f)]$ and $[H^*(2i\pi f)]$ the pair of diagonal complex matrix of structural frequency response function in terms of displacement; and $[S_{p^*}(f)]$ the spectral density matrix of generalized wind forces which can be computed by

$$[S_{p^*}(f)] = \int_0^H \int_0^H [\Phi(z_1)]^T [S_P(z_1, z_2, f)] [\Phi(z_2)] dz_1 dz_2, \tag{A.2}$$

where z_1 and z_2 are the dummy space variables; $[\Phi(z_1)]$ the mode shape matrix; and $[S_P(z_1, z_2, f)]$ the spectral density matrix of the aerodynamic forces, diagonal elements are auto-correlations and off-diagonals are cross-correlation of the aerodynamic forces. From (A.2), to calculate the generalized forces, information of the correlation structures of the aerodynamic forces on the building surface is

needed. Usually, this information is either unavailable unless the pressure-type wind tunnel test is employed, or hard to be proceeded for an actual wind engineering application due to significant efforts in data processing. On the other hand, a relationship can be employed to obtain the generalized wind loads by considering special structural mode shapes. Taking the sway mode as an example, the generalized wind load has the following relationship with the base moments in terms of PSD when the building has a linear mode shape in these directions:

$$S_{p^*}(f)_{D,L} = S_M(f)_{D,L}/H^2, \quad (\text{A.3})$$

where $S_{p^*}(f)$ is the PSD of generalized wind loads in fundamental modes; and $S_M(f)$ the PSD of aerodynamic BBMs. A similar relationship exists for the torsional direction by assuming a uniform mode shape. When buildings really have these kinds of mode shape, only very limited aerodynamic force information, i.e., the auto- and cross-correlations of the base moments, are needed to evaluate the wind-induced response. For buildings with mode shapes other than those assumed, mode shape corrections can be introduced to account for this departure. Usually, the mode shape correction depends on both the mode shape and the parameters describing the aerodynamic pressure field on the building surfaces. Given the mode shape correction, the PSD of the generalized displacement response can be obtained by using the base moment information

$$S_{\xi^*}(f) = \eta_{p^*} \cdot \frac{S_M(f)/H^2}{(2\pi f_1)^2 \cdot m_1^{*2}} \cdot |H_1(f)|^2, \quad (\text{A.4})$$

where η_{p^*} is the mode shape correction for the generalized wind loads; $m_1^* = \int_0^H m(z)\varphi_1(z) dz$ the generalized mass in the first mode; $\varphi_1(z) = (z/H)^\beta$ the mode shape in the first mode; β the mode shape exponent; $|H_1(f)|^2 = \{[1 - (f/f_1)^2]^2 + (2\zeta_1(f/f_1))^2\}^{-1}$ the structural transfer function in the first mode; and ζ_1 the critical structural damping ratio. Once the displacement response is available, the ESWL can be obtained. For example, the resonant ESWL component can be represented in terms of the inertial force. Using the ESWL, all wind load effects can be estimated using a simple static analysis. Similar analysis procedures can be developed for the torsional direction with an appropriate mode shape correction.

References

- [1] A.G. Davenport, Gust loading factors, *J. Struct. Div. ASCE* 93 (3) (1967) 11–34.
- [2] E. Simiu, R. Scanlan, *Wind Effects on Structures: Fundamentals and Applications to Design*, 3rd Edition, Wiley, New York, 1996.
- [3] J.D. Holmes, *Wind Loading on Structures*, SPON Press, London, 2001.
- [4] G. Solari, Gust buffeting. I: peak wind velocity and equivalent pressure, *J. Struct. Eng. ASCE* 119 (2) (1993) 365–382.
- [5] K. Gurley, A. Kareem, Gust loading factor for tension leg platforms, *Appl. Ocean Res.* 15 (3) (1993) 137–154.
- [6] G. Solari, Gust buffeting. II: dynamic along-wind response, *J. Struct. Eng. ASCE* 119 (2) (1993) 383–397.
- [7] Australian Standards, SAA Loading code, part 2—wind forces, AS1170.2-89, 1989.

- [8] American Concrete Institute, Standard practice for the design and construction of cast-in-place reinforced concrete chimneys, ACI307-88, ACI Detroit, 1988.
- [9] Y. Zhou, A. Kareem, M. Gu, Gust loading factors for design applications, Proceedings of the 10th ICWE, Copenhagen, Denmark, 1999, pp. 169–176.
- [10] Y. Zhou, A. Kareem, M. Gu, Equivalent static buffeting wind loads on structures, *J. Struct. Eng.* ASCE 126 (8) (2000) 989–992.
- [11] A.G. Davenport, Missing links in wind engineering, Proceedings of the 10th ICWE, Copenhagen, Denmark, 1999, pp. 1–8.
- [12] C. Drybre, S.O. Hansen, *Wind Loads on Structures*, Wiley, New York, 1997.
- [13] X. Chen, A. Kareem, Equivalent static wind loads on structures, Proceedings of the 11th International Conference on Wind Engineering, Lubbock, TX, June 2–5, 2003.
- [14] M. Kasperski, Extreme wind load distributions for linear and nonlinear design, *Eng. Struct.* 14 (1992) 27–34.
- [15] Y. Zhou, A. Kareem, Gust loading factor: new model, *J. Struct. Eng.* ASCE 127 (2) (2001) 168–175.
- [16] American Society of Civil Engineers (ASCE), *Minimum design loads for buildings and other structures*, ASCE 7–98. Reston, VA, 2000.
- [17] Y. Zhou, A. Kareem, On the aerodynamic admittance functions of tall buildings, NatHaz Modeling Laboratory Technical Report, 2002.
- [18] G. Solari, A. Kareem, On the formulation of ASCE7-95 gust effect factor, *J. Wind Eng. Ind. Aerodyn.* 77–78 (1998) 673–684.
- [19] B.E. Lee, W.K. Ng, Comparisons of estimated dynamic along-wind responses, *J. Wind Eng. Ind. Aerodyn.* 30 (1988) 153–162.
- [20] A. Kareem, Synthesis of fluctuating along-wind loads on tall buildings, *J. Eng. Mech.* ASCE 112 (1) (1986) 121–125.
- [21] Y. Zhou, T. Kijewski, A. Kareem, Aerodynamic loads on tall buildings: an interactive database, *J. Struct. Eng.* ASCE 129 (3) (2003) 394–404.
- [22] A.G. Davenport, How can we simplify and generalize wind loads, *J. Wind Eng. Ind. Aerodyn.* 54/55 (1995) 657–669.
- [23] B.J. Vickery, The response of chimneys and tower-like structures to wind loading, A State of the Art in Wind Engineering, Ninth International Conference on Wind Engineering, New Delhi, India, 1995, pp. 205–233.
- [24] Y. Zhou, A. Kareem, Torsional load effects on buildings under wind, in: M. Elgaaly (Ed.), *Advanced Techniques in Structural Engineering*, Proceedings of the Structures Congress 2000, Philadelphia, PA, CD-Rom, ASCE, Reston, VA, 2000.
- [25] Y. Zhou, A. Kareem, 3D gust loading factors for wind load effects on tall buildings, NatHaz Modeling Laboratory Technical Report, 2002.
- [26] T. Kijewski, A. Kareem, Dynamic wind effects: a comparative study of provisions in codes and standards with wind tunnel data, *Wind Struct.* 1 (1) (1998) 77–109.
- [27] Y. Zhou, T. Kijewski, A. Kareem, Along-wind load effects on tall buildings: a comparative study of major international codes and standards, *J. Struct. Eng.* ASCE 128 (6) (2002) 788–796.
- [28] G. Piccardo, G. Solari, 3D wind excited response of slender structures: basic formulation, closed-form solution, applications, *J. Struct. Eng.* ASCE 126 (8) (2000) 936–943.
- [29] D.W. Boggs, N. Hosoya, L. Cochran, Sources of torsional wind loading on tall buildings, in: M. Elgaaly (Ed.), *Advanced Techniques in Structural Engineering*, Proceedings of the Structures Congress 2000, Philadelphia, PA, CD-Rom, ASCE, Reston, VA, 2000.
- [30] N. Isyumov, P.C. Case, Wind-induced torsional loads and response of buildings, in: M. Elgaaly (Ed.), *Advanced Techniques in Structural Engineering*, Proceedings of the Structures Congress 2000, Philadelphia, PA, CD-Rom, ASCE, Reston, VA, 2000.
- [31] NRCC, *User's Guide-NBC1995 Structural Commentaries (Part 4)*, 1996.
- [32] J. Xie, P.A. Irwin, Key factors for torsional wind response of tall buildings, in: M. Elgaaly (Ed.), *Advanced Techniques in Structural Engineering*, Proceedings of the Structures Congress 2000, Philadelphia, PA, CD-Rom, ASCE, Reston, VA, 2000.

- [33] Y. Zhou, A. Kareem, M. Gu, Mode shape corrections for wind load effects on tall buildings, *J. Eng. Mech. ASCE* 128 (1) (2002) 15–23.
- [34] D.W. Boggs, J.A. Peterka, Aerodynamic model tests of tall buildings, *J. Eng. Mech. ASCE* 115 (3) (1989) 618–635.
- [35] T. Tschanz, A.G. Davenport, The base balance technique for the determination of dynamic wind loads, *J. Wind Eng. Ind. Aerodyn.* 13 (1983) 429–439.
- [36] A. Kareem, Measurements of total dynamic loads from surface pressures, in: T.A. Reinhold (Ed.), *National Bureau of Standards, Proceedings, International Workshop on Wind Tunnel Modeling Criteria and Techniques*, Gaithersburg, Maryland, Cambridge University Press, Cambridge, 1982.
- [37] T.C.E. Ho, G.R. Lythe, N. Isyumov, Structural loads and responses from the integration of instantaneous pressure, In: A. Larsen, G.L. Larose, F.M. Livesey (Eds.), *Wind Engineering into the 21st Century*, A.A. Balkema, Rotterdam, Vol. 3, 1999.
- [38] Y. Zhou, A. Kareem, Aeroelastic balance, *J. Eng. Mech. ASCE* 129 (3) (2002) 283–292.
- [39] Architectural Institute of Japan, *Recommendations for loads on buildings*, 1996.
- [40] ENV 1991-2-4, EUROCODE 1: basis of design and actions on structures, Part 2.4: wind actions, 1994.
- [41] A. Kareem, Lateral-torsional motion of tall buildings to wind loads, *J. Struct. Eng. ASCE* 111 (11) (1985) 2749–2796.